the two-dimensional scattering pattern has to be recorded. For such applications, any type of point collimation can be used.

Slit and pinhole cameras. The simplest way to build a camera is to use two pairs of slits or pinholes at a certain distance apart (Kratky, 1982*a*; Holmes, 1982). The narrower the slits and the larger the distance between them, the smaller is the smallest attainable scattering angle (sometimes called the '*resolution*'). Parasitic scattering and difficult alignment are the main problems for all such systems (Guinier & Fournet, 1955). A slit camera that has been used very successfully is that of Beeman and co-workers (Ritland, Kaesberg & Beeman, 1950; Anderegg, Beeman, Shulman & Kaesberg, 1955). A rather unusual design is adopted in the slit camera of Stasiecki & Stuhrmann (1978), whose overall length is 50 m! A highly developed system is the ORNL 10 m camera at Oak Ridge (Hendricks, 1978).

Standard-size cameras for laboratory application are commercially available with different designs from various companies.

Bonse–Hart camera. The Bonse–Hart camera (Bonse & Hart, 1965, 1966, 1967) is based on multiple reflections of the primary beam from opposite sides of a groove in an ideal germanium crystal (collimator and monochromator). After penetrating the sample, the scattered beam runs through the groove of a second crystal (analyser). This selects the scattering angle. Rotation of the second crystal allows the measurement of the angle-dependent scattering function. The appealing feature of this design is that one can measure down to very small angles without a narrow entrance slit. The system is therefore favourable for the investigation of very large particles ($D > 350$ nm). For smaller particles, one obtains better results with block collimation (Kratky & Leopold, 1970).

Camera systems for synchrotron radiation. Small-angle scattering facilities at synchrotrons are built by the local staff and details of the construction are not important for the user in most cases. Descriptions of the instruments are available from the local contacts. These small-angle scattering systems are usually built with crystal monochromators and focusing mirrors (point collimation). All elements have to be operated under remote control for safety reasons. A review of the different instruments was published recently by Koch (1988).

2.6.1.5.2. *Detectors*

In this field, we are facing the same situation as we met for X-ray sources. The detectors for small-angle scattering experiments are the same as or slightly modified from the detectors used in crystallography. Therefore, it is sufficient to give a short summary of the detectors in the following; further details are given in Chapter 7.1. If we are not investigating the special cases of fully or partially oriented systems, we have to measure the dependence of the scattered intensity on the scattering angle, *i.e.* a one-dimensional function. This can be done with a standard gas-filled proportional counter that is operated in a sequential mode (Leopold, 1982), *i.e.* a positioning device moves the receiving slit and the detector to the desired angular position and the radiation detector senses the scattered intensity at that position. In order to obtain the whole scattering curve, a series of different angles must be positioned sequentially and the intensity readings at every position must be recorded. The system has a very high dynamic range, but – as the intensities at different angles are measured at different times – the stability of the primary beam is of great importance.

This drawback is eliminated in the parallel detection mode with the use of position-sensitive detectors. Such systems are in most cases proportional counters with sophisticated and expensive read-out electronics that can evaluate on-line the accurate position where the pulses have been created by the incoming radiation.

Two-dimensional position-sensitive detectors are necessary for oriented systems, but they also have advantages in the case of non-oriented samples when circular chambers are used or when integration techniques in square detectors lead to a higher signal at large scattering angles.

The simplest and cheapest two-dimensional detector is still film, but films are not used very frequently in small-angle scattering experiments because of limited linearity and dynamic range, and fog intensity.

Koch (1988) reviews the one- and two-dimensional detectors actually used in synchrotron small-angle scattering experiments. For a general review of detectors, see Hendrix (1985).

2.6.1.6. *Data evaluation and interpretation*

After having discussed the general principles and the basics of instrumentation in the previous subsections, we can now discuss how to handle measured data. This can only be a very short survey; a detailed description of data treatment and interpretation has been given previously (Glatter, 1982*a*,*b*).

Every physical investigation consists of three highly correlated parts: theory, experiment, and evaluation of data. The theory predicts a possible experiment, experimental data have to be collected in a way that the evaluation of the information wanted is possible, the experimental situation has to be described theoretically and has to be taken into account in the process of data evaluation *etc*. This correlation should be remembered at every stage of the investigation. Before we can start any discussion about interpretation, we have to describe the experimental situation carefully.

All the theoretical equations in the previous subsections correspond to ideal conditions as mentioned in the subsection on instrumentation. In real experiments, we do not measure with a point-like parallel and strictly monochromatic primary beam and our detector will have non-negligible dimensions. The finite size of the beam, its divergence, the size of the detector, and the wavelength distribution will lead to an instrumental broadening as in most physical investigations. The measured scattering curve is said to be *smeared* by these effects. So we find ourselves in the following situation.

The particle is represented by its PDDF $p(r)$. This function is not measured directly. In the scattering process it is Fourier-transformed into a scattering function $I(h)$ [equation (2.6.1.9)]. This function is smeared by the broadening effects and the final *smeared* scattering function $I_{\rm exp}(h)$ is measured with a certain experimental error $\sigma(h)$. In the case of polydisperse systems, the situation is very similar; we start from a size-distribution function $D(R)$ and have a different transformation [equations (2.6.1.54), (2.6.1.55)], but the smearing problem is the same.

2.6.1.6.1. *Primary data handling*

In order to obtain reliable results, we have to perform a series of experiments. We have to repeat the experiment for every sample, to be able to estimate a mean value and a standard deviation at every scattering angle. This experimentally determined standard deviation is often much higher than the standard deviation simply estimated from counting statistics. A blank experiment (cuvette filled with solvent only) is necessary to be able to subtract background scattering coming from the instrument and from the solvent (or *matrix* in the case of solid samples). Finally, we have to perform a series of such

experiments at different concentrations to extrapolate to zero concentration (elimination of interparticle interferences).

If the scattering efficiency of the sample is low (low contrast, small particles), it may be necessary to measure the outer part of the scattering function with a larger entrance slit and we will have to merge different parts of the scattering function. The intensity of the instrument (primary beam) should be checked before each measurement. This allows correction (normalization) for instabilities.

It is therefore necessary to have a so-called primary data-handling routine that performs all these preliminary steps like averaging, subtraction, normalization, overlapping, concentration extrapolation, and graphical representation on a graphics terminal or plotter. In addition, it is helpful to have the possibility of calculating the Guinier radius, Porod extrapolation [equations (2.6.1.24)], invariant, *etc*. from the raw data.

When all these preliminary steps have been performed, we have a smeared particle-scattering function $I_{\rm exp}(h)$ with a certain statistical accuracy. From this data set, we want to compute $I(h)$ and $p(r)$ [or $D(R)$] and all our particle parameters. In order to do this, we have to *smooth* and *desmear* our function $I_{\rm exp}(h)$. The smoothing operation is an absolute necessity because the desmearing process is comparable to a differentiation that is impossible for noisy data. Finally, we have to perform a Fourier transform (or other similar transformation) to invert equations (2.6.1.9) or (2.6.1.54), (2.6.1.55). Before we can discuss the desmearing process (collimation error correction) we have to describe the smearing process.

2.6.1.6.2. *Instrumental broadening – smearing*

These effects can be separated into three components: the two-dimensional geometrical effects and the wavelength effect. The geometrical effects can be separated into a slit-length (or slit-height) effect and a slit-width effect. The slit length is perpendicular to the direction of increasing scattering angle; the corresponding weighting function is usually called $P(t)$. The slit width is measured in the direction of increasing scattering angles and the weighting function is called $Q(x)$. If there is a wavelength distribution, we call the weighting function $W(\lambda')$ where $\lambda' = \lambda/\lambda_0$ and λ_0 is the reference wavelength used in equation (2.6.1.2). When a conventional X-ray source is used, it is sufficient in most cases to correct only for the $K\beta$ contribution. Instead of the weighting function $W(\lambda')$ one only needs the ratio between $K\beta$ and $K\alpha$ radiation, which has to be determined experimentally (Zipper, 1969). One or more smearing effects may be negligible, depending on the experimental situation.

Each effect can be described separately by an integral equation (Glatter, 1982*a*). The combined formula reads

$$\bar{I}_{\rm exp}(h) = 2 \int_{-\infty}^{\infty} \int_{0}^{\infty} \int_{0}^{\infty} Q(x)P(t)W(\lambda') \times I\left(\frac{[(m-x)^2 + t^2]^{1/2}}{\lambda'}\right) {\rm d}\lambda'\ {\rm d}t\ {\rm d}x. \qquad (2.6.1.56)$$

This threefold integral equation cannot be solved analytically. Numerical methods must be used for its solution.

2.6.1.6.3. *Smoothing, desmearing, and Fourier transformation*

There are many methods published that offer a solution for this problem. Most are referenced and some are reviewed in the textbooks (Glatter, 1982*a*; Feigin & Svergun, 1987). The *indirect transformation method* in its original version (Glatter, 1977*a*,*b*, 1980*a*,*b*) or in modifications for special applications (Moore, 1980; Feigin & Svergun, 1987) is a well established method used in the majority of laboratories for different applications. This procedure solves the problems of smoothing, desmearing, and Fourier transformation [inversion of equations (2.6.1.9) or (2.6.1.54), (2.6.1.55)] in one step. A short description of this technique is given in the following.

Indirect transformation methods. The *indirect transformation method* combines the following demands: single-step procedure, optimized general-function system, weighted least-squares approximation, minimization of termination effect, error propagation, and consideration of the physical smoothing condition given by the maximum intraparticle distance. This smoothing condition requires an estimate $D_{\rm max}$ as an upper limit for the largest particle dimension:

$$D_{\rm max} \geq D. \qquad (2.6.1.57)$$

For the following, it is not necessary for $D_{\rm max}$ to be a perfect estimate, but it must not be smaller than D.

As $p(r) = 0$ for $r \geq D_{\rm max}$, we can use a function system for the representation of $p(r)$ that is defined only in the subspace $0 \leq r \leq D_{\rm max}$. A linear combination

$$p_A(r) = \sum_{\nu=1}^{N} c_\nu \varphi_\nu(r) \qquad (2.6.1.58)$$

is used as an approximation to the PDDF. Let N be the number of functions and c_ν be the unknowns. The functions $\varphi_\nu(r)$ are chosen as cubic B splines (Greville, 1969; Schelten & Hossfeld, 1971) as they represent smooth curves with a minimum second derivative.

Now we take advantage of two facts. The first is that we know precisely how to calculate a smeared scattering function $\bar{I}(h)$ from $I(h)$ [equation (2.6.1.56)] and how $p(r)$ or $D(R)$ is transformed into $I(h)$ [equations (2.6.1.9) or (2.6.1.54), (2.6.1.55)], but we do not know the inverse transformations. The second fact is that all these transformations are linear, *i.e*. they can be applied to all terms in a sum like that in equation (2.6.1.58) separately. So it is easy to start with our approximation in real space [equation (2.6.1.58)] taking into account the *a priori* information $D_{\rm max}$. The approximation $I_A(h)$ to the ideal (unsmeared) scattering function can be written as

$$I_A(h) = \sum_{\nu=1}^{N} c_\nu \Psi_\nu(h), \qquad (2.6.1.59)$$

where the functions $\Psi_\nu(h)$ are calculated from $\varphi_\nu(r)$ by the transformations (2.6.1.9) or (2.6.1.54), (2.6.1.55), the coefficients c_ν remain unknown. The final fit in the smeared, experimental space is given by a similar series

$$\bar{I}_A(h) = \sum_{\nu=1}^{N} c_\nu \chi_\nu(h), \qquad (2.6.1.60)$$

where the $\chi_\nu(h)$ are functions calculated from $\psi_\nu(h)$ by the transform (2.6.1.56). Equations (2.6.1.58), (2.6.1.59), and (2.6.1.60) are similar because of the linearity of the transforms. We see that the functions $\chi_\nu(h)$ are calculated from $\varphi_\nu(r)$ in the same way as the data $\bar{I}_{\rm exp}(h)$ were produced by the experiment from $p(r)$. Now we can minimize the expression

$$L = \sum_{k=1}^{M} [\bar{I}_{\rm exp}(h_k) - \bar{I}_A(h_k)]^2 / \sigma^2(h_k), \qquad (2.6.1.61)$$

where M is the number of experimental points. Such *least-squares problems* are in most cases *ill conditioned, i.e*. additional stabilization routines are necessary to find the best

solution. This problem is far from being trivial, but it can be solved with standard routines (Glatter, 1977*a*,*b*; Tikhonov & Arsenin, 1977).

The whole process of data evaluation is shown in Fig. 2.6.1.14. Similar routines cannot be used in crystallography (periodic structures) because there exists no estimate for $D_{\max}$ [equation (2.6.1.57)].

Maximum particle dimension. The sampling theorem of Fourier transformation (Shannon & Weaver, 1949; Bracewell, 1986) gives a clear answer to the question of how the size of the particle D is related to the smallest scattering angle h_1. If the scattering curve is observed at increments $\Delta h \leq h_1$ starting from a scattering angle h_1, the scattering data contain, at least theoretically, the full information for all particles with maximum dimension D

$$D \leq \pi/h_1. \tag{2.6.1.62}$$

The first application of this theorem to the problem of data evaluation was given by Damaschun & Pürschel (1971*a*,*b*). In practice, one should always try to stay below this limit, *i.e.*

$$h_1 < \pi/D \quad \text{and} \quad \Delta h \ll h_1, \tag{2.6.1.63}$$

taking into account the loss of information due to counting statistics and smearing effects. An optimum value for $\Delta h = \pi/(6D)$ is claimed by Walter, Kranold & Becherer (1974).

Information content. The number of *independent* parameters contained in a small-angle scattering curve is given by

$$N_{\max} \leq h_2/h_1, \tag{2.6.1.64}$$

with h_1 and h_2 being the lower and upper limits of h. In practice, this limit certainly depends on the statistical accuracy of the data. It should be noted that the number of functions N in equations (2.6.1.58) to (2.6.1.60) may be larger than $N_{\max}$ because they are not independent. They are correlated by the stabilization routine. An example of this problem can be found in Glatter (1980*a*).

Resolution. There is no clear answer to the question concerning the smallest structural details, *i.e.* details in the $p(r)$ function that can be recognized from an experimental scattering function. The limiting factors are the maximum scattering angle h_2, the statistical error $\sigma(h)$, and the weighting functions $P(t)$, $Q(x)$, and $W(\lambda')$ (Glatter, 1982*a*). The resolution of standard experiments is not better than approximately 10% of the maximum dimension of the particle for a monodisperse system. In the case of polydisperse systems, resolution can be defined as the minimum relative peak distance that can be resolved in a bimodal distribution. We know from simulations that this value is of the order of 25%.

Special transforms. The PDDF $p(r)$ or the size distribution function $D(R)$ is related to $I(h)$ by equations (2.6.1.9) or (2.6.1.54), (2.6.1.55). In the special case of particles elongated in one direction (like cylinders), we can combine equations (2.6.1.41) and (2.6.1.43) and obtain

$$I(h) = 2\pi^2 L \int_0^\infty p_c(r) \frac{J_0(hr)}{h}\, \mathrm{d}r. \tag{2.6.1.65}$$

This Hankel transform can be used in the indirect transformation method for the calculation of $\psi_\nu(h)$ in (2.6.1.59). Doing this, we immediately obtain the PDDF of the cross section $p_c(r)$ from the smeared experimental data. It is not necessary to know the length L of the particle if the results are not needed on an absolute scale. For this application, we only need the information that the scatterers are elongated in one direction with a constant cross section. This information can be found from the overall PDDF of the particle or can be *a priori* information from other experiments, like electron microscopy. The estimate for the maximum dimension $D_{\max}$ (2.6.1.57) is related to the cross

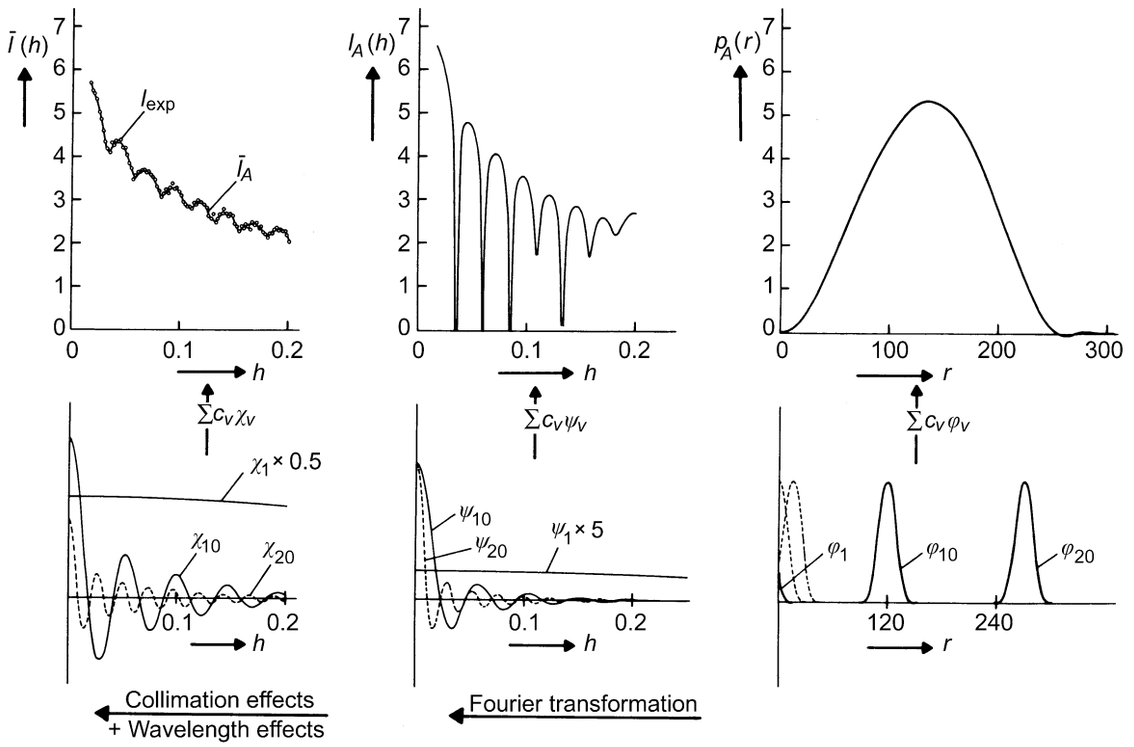

Fig. 2.6.1.14. Function systems $\varphi_\nu(r)$, $\Psi_\nu(h)$, and $\chi_\nu(h)$ used for the approximation of the scattering data in the indirect transformation method.

section in this application, *i.e.* the maximum dimension of the cross section must not be larger than $D_{\max}$.

The situation is quite similar for flat particles. If we combine (2.6.1.47) and (2.6.1.49), we obtain

$$I(h) = 4\pi A \int_0^\infty p_t(r) \frac{\cos(hr)}{h^2}\, \mathrm{d}r, \qquad (2.6.1.66)$$

$p_t(r)$ being the distance distribution function of the thickness. We have to check that the particles are flat with a constant thickness with maximum thickness $T \leq D_{\max}$. A is the area of the particles and would be needed only for experiments on an absolute scale.

2.6.1.6.4. *Direct structure analysis*

It is impossible to determine the three-dimensional structure $\rho(\mathbf{r})$ directly from the one-dimensional information $I(h)$ or $p(r)$. Any direct method needs additional *a priori information* – or assumptions – on the system under investigation. If this information tells us that the structure only depends on one variable, *i.e.* the structure is in a general sense *one dimensional*, we have a good chance of recovering the structure from our scattering data.

Examples for this case are particles with spherical symmetry, *i.e.* ρ depends only on the distance r from the centre, or particles with cylindrical or lamellar symmetry where ρ depends only on the distance from the cylinder axis or from the distance from the central plane in the lamella. We will restrict our discussion here to the spherical problem but we keep in mind that similar methods exist for the cylindrical and the lamellar case.

Spherical symmetry. This case is described by equations (2.6.1.51) and (2.6.1.52). As already mentioned in §2.6.1.3.2.2, we can solve the problem of the calculation of $\rho(r)$ from $I(h)$ in two different ways. We can calculate $\rho(r)$ *via* the distance distribution function $p(r)$ with a *convolution square-root* technique (Glatter, 1981; Glatter & Hainisch, 1984). The other way goes through the amplitude function $A(h)$ and its Fourier transform. In this case, one has to find the right phases (signs) in the square-root operation $\{A(h) = \pm[I(h)^{1/2}]\}$.The *box-function refinement* method by Svergun, Feigin & Schedrin (1984) is an iterative technique for the solution of the phase problem using the *a priori* information that $\rho(r)$ is equal to zero for $r \geq R_{\max}$ ($D_{\max}/2$). The same restriction is used in the convolution square-root technique. Under ideal conditions (perfect spherical symmetry), both methods give good results. In the case of deviations from spherical symmetry, one obtains better results with the convolution square-root technique (Glatter, 1988). With this method, the results are less distorted by non-spherical contributions.

Multipole expansions. A wide class of homogeneous particles can be represented by a boundary function that can be expanded into a series of spherical harmonics. The coefficients are related to the coefficients of a power series of the scattering function $I(h)$, which are connected with the moments of the PDDF (Stuhrmann, 1970*b*,*c*; Stuhrmann, Koch, Parfait, Haas, Ibel & Crichton, 1977). Of course, this expansion cannot be unique, *i.e.* for a certain scattering function $I(h)$ one can find a large variety of possible expansion coefficients and shapes. In any case, additional *a priori* information is necessary to reduce this number, which in turn influences the convergence of the expansion. Only compact, globular structures can be approximated with a small number of coefficients.

This concept is not restricted to the determination of the shape of the particles. Even inhomogeneous particles can be described using all possible radial terms in a general expansion (Stuhrmann, 1970*a*). The information content can be increased by contrast variation (Stuhrmann, 1982), but in any event one is left with the problem of how to find additional *a priori* information in order to reduce the possible structures. Any type of symmetry will lead to a considerable improvement. The case of axial symmetry is a good example. Svergun, Feigin & Schedrin (1982) have shown that the quality of the results can be further improved when upper and lower limits for $\rho(\mathbf{r})$ can be used. Such limits can come from a known chemical composition.

2.6.1.6.5. *Interpretation of results*

After having used all possible data-evaluation techniques, we end up with a desmeared scattering function $I(h)$, the PDDF $p(r)$ or the size-distribution function $D(R)$, and some special functions discussed in the previous subsections. Together with the particle parameters, we have a data set that can give us at least a rough classification of the substance under investigation.

The interpretation can be performed in reciprocal space (scattering function) or in real space (PDDF *etc*.). Any symmetry can be detected more easily in reciprocal space, but all other structural information can be found more easily in real space (Glatter, 1979, 1982*b*).

When a certain structure is estimated from the data and from *a priori* information, one has to test the corresponding model. That means one has to find the PDDF and $I(h)$ for the model and has to compare it with the experimental data. Every model that fits within the experimental errors can be true, all that do not fit have to be rejected. If the model does not fit, it has to be refined by trial and error. In most cases, this process is much easier in real space than in reciprocal space. Finally, we may end up with a set of possible structures that can be correct. Additional *a priori* information will be necessary to reduce this number.

2.6.1.7. *Simulations and model calculations*

2.6.1.7.1. *Simulations*

Simulations can help to find the limits of the method and to estimate the systematic errors introduced by the data-evaluation procedure. Simulations are performed with exactly known model systems (test functions). These systems should be similar to the structures of interest. The model data are transformed according to the special experimental situation (collimation profiles and wavelength distribution) starting from the theoretical PDDF (or scattering function). '*Experimental data points*' are generated by sampling in a limited h range and adding statistical noise from a random-number generator. If necessary, a certain amount of background scattering can also be added. This simulated data set is subjected to the data-evaluation procedure and the result is compared with the starting function. Such simulation can reveal the influence of each approximation applied in the various evaluation routines.

On the other hand, simulations can also be used for the optimization of the experimental design for a special application. The experiment situation is characterized by several contradictory effects: a large width for the functions $P(t)$, $Q(x)$, and $W(\lambda')$ leads to a high statistical accuracy but considerable smearing effects. The quality of the results of the desmearing procedure is increased by high statistical accuracy, but decreased by large smearing effects. Simulations can help to find the optimum for a special application.